Extraction and Characterization of *Cayratia pedata (lam.) gagnep* Fiber

P. Senthamaraikannan[1*], Indran Suyambulingam[1], S. S. Saravanakumar[2], Sikiru O. Ismail[3,*], Suchart Siengchin[4]

[1]Sophisticated Testing and Instrumentation Centre (STIC), Department of Mechanical Engineering, Alliance School of Applied Engineering, Alliance University, Bengaluru 562106, Karnataka, India.

[2]Department of Mechanical Engineering, K. S. Rangasamy College of Technology, KSR Kalvi Nagar, Tiruchengode, Tamil Nadu, India

[3]Department of Engineering, School of Engineering and Computer Science, Centre for Engineering Research, University of Hertfordshire, Hatfield, Hertfordshire AL10 9AB, England, United Kingdom

[4]Natural Composites Research Group Laboratory, Department of Materials and Production Engineering, The Sirindhorn International Thai-German School of Engineering (TGGS), King Mongkut's University of Technology North Bangkok (KMUTNB), Bangkok, Thailand

******Corresponding authors***:** P. Senthamaraikannan, E-mail:senthamaraikannan1991@gmail.com
S. O. Ismail, E-mail: s.ismail3@herts.ac.uk

Abstract

The quest for sustainability, renewability, manufacturing cost efficiency and environmental friendliness in composite science and technology is ongoing, due to numerous benefits. In this research, mature stems of the *Cayratia pedata (lam.) gagnep* (CPG) plant were harvested, and their long fibers were extracted through water retting and comprehensively characterized as a potential reinforcement for polymer matrix composites (PMCs). The results showed that *Cayratia pedata (lam.) gagnep* fibers (CPGF) with a lower density of 1158.00±52 kg/m³ supported fabrication of PMCs with less weight and high strengths. Hemicellulose and

cellulose of 16.47±3.26 and 65.21±5.31 wt.% were obtained from CPGF via chemical analysis, respectively. Its crystallinity index of 67.84% confirmed comparatively higher crystalline material. Fourier transform infrared (FTIR) analysis identified the different functional groups in CPGF. The thermal degradation analysis of CPGF demonstrated its suitability as a reinforcing material in PMCs up to a fabrication temperature of 250 ºC. The higher kinetic activation energy of CPGF at 97.40 kJ/mol also established its improved thermal stability. The outer shell of the CPGF had debris and non-cellulosic materials, as examined through a scanning electron microscope (SEM). Due to impurities, lignin and hemicellulose, untreated fibers were smoother than desired. The mean tensile strength of CPGF was 424.40±24.45 MPa. Weibull distribution was employed to statistically investigate the single CPGF tensile properties. In summary, it can be concluded that CPGF is a better alternative, sustainable, renewable, low-cost and environmentally friendly reinforcing material when compared extensively with several similar plant fibers.

Keywords: *Cayratia pedata (lam.) gagnep* fiber (CPGF), Chemical analysis, Crystallinity index, Thermal degradation, Surface roughness.

1. Introduction

Environmental protection agencies are making rules and guidelines worldwide to lessen environmental damage. These laws and regulations insist on reduced consumption of non-biodegradable materials (Sanjay et al. 2018). Several sectors, such as biomedical, automobile, defence, building and packaging, use synthetic fiber-reinforced polymer (FRP) composites. The use of synthetic FRP composite materials is difficult to avoid, because of their advantages. They are cheaper, lightweight, easy to fabricate, non-corrosive and simple to handle (Marichelvam et al. 2021; Saha et al. 2023). On the other hand, synthetic FRP composites damage environments. This drives investigation into developing eco-friendly materials to

replace synthetic FRP composites (Binoj et al. 2016; Saha et al. 2021a). Synthetic fibers, such as rayon, spandex, acrylic, polyester and nylon can be substituted with plant fibers. Therefore, studies on plant FRP composites and the quest to improve their properties and performances have attracted increasing interest in several industries.

Moreover, plant FRP composites are partially biodegradable. Generally, polymer matrix composites (PMCs) comprise a matrix and reinforcement (Mansingh et al. 2021). Therefore, the properties of composites depend on the matrix material, type of reinforcement and binding strength between the resin and fiber, which is commonly called fiber-matrix adhesion. The characteristics of plant fibers are determined by various factors. Among the vital factors is their chemical composition, particularly the quantity of cellulose present. Many factors influence the chemical constitution of the fiber (Kumar et al. 2020; Amutha and Senthilkumar 2021). These include, but are not limited to, maturity, grown environment, method of extraction and part of the plant. Soil nutrients, pH, temperature, humidity, rainfall, mineral content, salinity, sunlight intensity, environmental stresses, pests, pollutants and agricultural practices impact the fiber properties of plants grown in a given area. Various parts of the plants yield fibers, including bark, stem, root, leaf, aerial root and flower. Fibers extracted from the plant stems are preferred for composite reinforcement, since they yield lengthy fibers. The long fibers can make unidirectional and multi-directional mats (Senthamaraikannan and Kathiresan 2018a; Saha et al. 2021c). In addition to cellulose, plant fibers have a small quantity of amorphous fractions: hemicellulose, lignin and wax. Amorphous fractions influence the mechanical, thermal and crystalline properties; hence, fibers with minimal amorphous fractions are preferable (Moshi et al. 2019; Bharath et al. 2020; Kumar et al. 2022).

Two different types of plants yield cellulosic fibers. The first is plants cultivated for fiber extraction, such as sisal, flax and hemp, to mention but a few. The second is fibers from agricultural wastes, such as banana, coir and aerial root banyan fiber (Saha et al. 2021b; Kumar

and Saha 2024). The need for plant fiber is increasing, because of its utilization in different sectors. This increase in demand stimulates researchers to explore other plant fibers. Various plant fibers, including *Derris scandens* stem, *Rosa hybrida* bark, Cissus vitiginea stem, *Mariscus ligularis* fibers and *Bambusa tulda*, were extracted recently. Studies on their suitability for reinforcement in polymers to produce biocomposites have been widely reported (Chakravarthy et al. 2020; Perumal and Sarala 2020; Saha and Kumari 2022; Garriba and Siddhi Jailani 2023; Shibly et al. 2024). In a bid to discover another plant fiber, this work attempted to extract the plant fiber from the stems of *Cayratia pedata (lam.) gagnep* (CPG) plant. CPG exists in different parts of the world, especially in India, Myanmar, Sri Lanka, Thailand, Australia, Malaysia, Indonesia and Newland.

Cayratia pedata (lam.) gagnep (CPG) is common in various regions of India, including Kerala, Tamil Nadu and Andhra Pradesh. It is typically found in natural habitats, such as moist deciduous and semi-evergreen forest. Locally, the plant is referred to as "Kattu Pirandai" and "Panni Kodi" and is a climber that attaches itself to the adjacent vegetation with tendrils. CPG is a climbing plant that can grow over 20 meters long. Among other similar plants, CPG plant was selected for fiber extraction, because it is highly available in various parts of the globe, yields around 60 wt.% of fiber, its water retting period is only 10 days and requires no unique tool, long fibers of around 10 meters can be extracted, supporting possibility of making unidirectional and multi-directional fiber mats. More importantly, CPGF has not been extracted from its plant and comprehensively characterized as a potential reinforcement within a biocomposite material, considering several existing relevant studies. Therefore, this study bridged the research gap in biocomposite science and technology. After extracting CPGF, fundamental fiber properties were extensively investigated within the scope of this research through appropriate techniques to establish its application as a potential natural reinforcement or biofiber for sustainable, renewable, environmentally friendly and low-cost biocomposite structures.

2. Materials and methods

2.1 Fiber extraction

Matured stalks of CPG plants (commonly known as Birdfoot Grape-Vine), existing near Kottaimalai Falls (Geographical coordinates: 9.771299631204895, 77.65746692522843), Saturagiri forest area, T. Krishnapuram were manually removed from their plants. The stems were soaked for 10 days (Sanjay et al. 2019) at around 25 ºC. After 10 days, unwanted flesh surrounding the fibers was retted, and the fibers remained alone. The remaining fibers were cleansed, using running water and then demineralized water to remove unwanted impurities on the fibers. Around 60% of the fiber is retained after the water-retting process. The cleaned CPGF were dried in daylight for three days to undergo dehydration and then packed in zipped polyethene packaging in preparation for characterization. The extraction process is depicted in Fig. 1.

Fig. 1. (a) CPG plant, (b) stem of the plant, (c) water retting and (d) extracted fibers.

2.2 Estimation of diameter and density of CPGF

The diameters of the fibers influence the mechanical characteristics of biofibers and developed FRP composites. This research employed an optical microscope (Carl Zeiss AG, Germany) to measure plant fiber diameters (Belouadah et al. 2021), because of its accuracy. Cellulosic fiber diameters vary slightly from fiber to fiber, because of variations in the maturity of plants. The diameter of many plant fibers varies from place to place. Therefore, measuring the diameter of at least 20 single fibers was necessary to find the average diameter of the plant fibers. The diameter was measured in four different regions on a fiber, and the mean value was obtained and recorded. Plant fibers generally possess low weight. A liquid-based specific gravity measurement bottle was an appropriate device to estimate the density of the plant fibers (Mohan et al. 2022a). Toluene, with a known density of 866 kg/m³, was used in this experiment. Five trials were taken, and the average density value was reported.

2.3 Estimation of chemical constitutions of CPGF

Plant fibers comprise various chemical constituents: cellulose, hemicellulose, lignin and wax. Different plant fibers possess different quantities of chemical components. The chemical compositions can be quantified, using the following unique techniques.

- The cellulose content of CPGF was estimated, using a method established by Kurschner and Hoffer (Kurschner K and Hoffer A 1933).
- Hemicellulose in the CPGF was determined through the neutral detergent fiber technique (Jaiswal et al. 2022).
- Following the APPITA P11s-78 standard, the lignin content of the CPGF was determined (Jaiswal et al., 2022).
- Conrad's method was used to determine the wax fraction in the fiber (Conrad 1944).
- The ash content of the CPGF was estimated following TAPPI specifications.

- Mettler Toledo-made (HS153-Model) moisture measuring device is commonly utilized in the textile industry. Hence, it was employed to determine moisture content in CPGF.

Tests were taken five times to find the accurate values, and mean values were reported.

2.4 Crystallographic study of CPGF

The X'Pert-Pro- (PANalytical, Netherlands) X-ray diffraction (XRD) machine was used for the crystallographic analysis of CPGF. Initially, CPGF fiber was prepared with the help of mixture grinder, and it was placed in the sample holder. The X-rays generated by the machine were directed at the CPGF powder and diffracted upon collision with the CPGF particles. The diffracted X-rays were detected by a moving X-ray detector between 2θ = 10º and 60º. The movement of the X-ray detector was restricted to 2θ = 0.02º per step. The determination of the crystallinity index (CI) of the CPGF was accomplished, using the traditional peak height measurement method (Eq. (1))(Segal et al. 1959).

$$CI = \frac{Y_{22.75} - Y_{18.66}}{Y_{22.75}} X\ 100 \qquad (1)$$

$Y_{22.75}$ denotes the intensity of the crystalline peak, and $Y_{18.66}$ represents amorphous region, at the minimum in the intensity between the 110 and 200 peaks, at about 18.66.

By substituting values in the following mathematical relation, the crystalline size (CS) of the CPGF was computed, using Eq. (2) (French and Santiago Cintrón 2013).

$$CS_{22.475} = \frac{0.89\,\lambda}{FWHM_{22.75}\cos\theta} \qquad (2)$$

where λ represents 1.54178 Å and $FWHM_{22.75}$ stands for full-width at half-maximum of a predominated peak visualized at 2θ = 22.75°, as later shown in Fig. 3.

2.5 Identification of chemical functional groups in CPGF

Fourier transform infrared (FTIR) analysis is a suitable approach for categorizing chemical functional groups of plant fibers. JASCO-6300 model (Japan) equipment was utilized in this investigation. Powder CPGF and potassium bromide (KBr) were thoroughly mixed in a ratio of 1:10. A thin film was formed from the CPGF and KBr blend, using a manual press (Michell 1993). Infrared light was sent through the film, and transmitted light was recorded. A resolution of 4 cm^{-1} was maintained throughout the test. A graph was generated between the percentage of normalized transmission and wavenumber. From the graph, wavenumbers of notable peaks were marked.

2.6 Thermal degradation behavior of CPGF

To select appropriate composite manufacturing techniques, machining methods and relevant composite applications, it is necessary to investigate into the thermal degradation behavior of the plant fibers, as subsequently elucidated.

2.6.1 Thermogravimetric analysis

Thermogravimetric analysis (TGA) is a well-known method for determining the thermal degradation profile of plant fibers. Specific temperatures and conditions are employed in TGA to measure weight loss, ensure data consistency, control decomposition rates, prevent unwanted chemical reactions, and identify thermal stability. These standardized techniques are indispensable for assessing and utilising plant fibers in various applications, as they offer comprehensive thermal degradation profiles. Hence, EXSTAR- 6300 TGA machine (Seiko Instruments Inc. (SII), Japan) was employed to perform the analysis. A small amount of CPGF was placed in an alumina crucible. The alumina crucible was connected to a sensitive weighing machine. By applying heat from ambient temperature to 800 ºC, the temperature of the crucible was elevated. A constant rate of heating under 10 ºC/min was used. An inert gas was passed to

avoid unsolicited chemical reactions during the heating. In this experiment, nitrogen (N_2) was circulated with a mass flow rate of 200 ml/min (Felix Sahayaraj et al. 2022). The weighing machine recorded the fiber weight for every 10 ºC/min temperature increase.

2.6.2 Calculation of kinetic activation energy

An alternative method for assessing the thermal performance of plant fibers is by computing their kinetic activation energy (E_a). The kinetic activation energy of the plant fibers denotes the thermal energy required to initiate the thermal degradation process. Therefore, the E_a value was determined, using an easy graphic approach developed by Broido (Broido 1969). At the outset, Broido's curve was constituted, and its slope was computed with the aid of the Origin Pro software. The slope value was applied to Eq. (3) to obtain the final E_a value.

$$ln\left[ln\left(\frac{1}{y}\right)\right] = -\left(\frac{E_a}{8.32}\right)\left[\left(\frac{1}{T}\right) + Reaction\ rate\ constant\right] \quad (3)$$

where T represents the temperature of the CPGF on the Kelvin scale, and y denotes the proportion relative to the weight of the CPGF at x temperature and the weight of the CPGF before the start of the experimentation.

2.6.3 Differential thermal analysis

The TGA machine also recorded the differential thermal analysis (DTA) data points in this analysis. Using the DTA data, various properties, such as moisture loss and degradation of different chemical constitutions in the fiber, were obtained by identifying exothermic or endothermic reactions (Gedik 2021).

2.7 Surface investigation

The strength of bonding between reinforcement and resin is a crucial determinant of the mechanical properties of composites. The surface morphology of the plant fibers majorly influences this adhesion. Impurity-free rough surfaces are preferable for composite fabrication.

2.7.1 Scanning electron microscopic analysis

The examination of the outer surface of the CPGF was carried out by employing a FEG-200 model (FEI Quanta-Make, United States) scanning electron microscope (SEM). SEM images were captured with magnifications of 250, 500, 1000 and 1500x. Acceleration voltage and pressure were maintained throughout the experiment at 15 kV and 50 Pa, respectively. It was necessary to provide a coating, using conductive materials to obtain clear images of non-conductive materials. Hence, the gold coating was applied on the CPGF surfaces (Saravanan et al. 2022).

2.7.2 Energy dispersive X-ray analysis of CPGF

The FEI Quanta-Make (United States), FEG-200 model SEM machine was used for the energy dispersive X-ray (EDX) analysis. It was an advanced machine with an EDX attachment. The EDX attachment could record the different elements spread over the fiber exterior. During the EDX experimentation, acceleration voltage of 20.0 kV was maintained, and magnification was fixed at around 600x (Boominathan et al. 2023).

2.7.3 Atomic force microscopy analysis

SEM analysis provided qualitative information about the fiber surfaces, whereas atomic force microscopy (AFM) analysis presented qualitative and quantitative data. The analysis used a Park-Make (South Korea) XE-70 type AFM analyzer. The experiment was carried out in a non-conduction mode. Initially, three-dimensional (3D) and two-dimensional (2D) images

were captured. Surface topographical parameters were obtained, using an XEI image processing software (Narayana Perumal et al. 2023).

2.8 Mechanical testing

The tensile strength of individual plant fibers is a critical determinant in establishing the mechanical characteristics of composites reinforced with plant fibers. Therefore, utilizing a Zwick/Roell (Germany) testing machine with a load cell of 2.5 kN, CPGF single fiber tensile testing was performed. Due to the change in the diameter of each fiber, it was necessary to test at least 20 fibers. A total of 20 single fibers with gauge lengths of 50 mm were taken for experimentation. Tensile properties of CPGF were statistically analyzed (Weibull distribution), using Minitab 18 software (Vijay et al. 2019). The Weibull distribution was selected to analyze plant fiber mechanical properties, because of its flexibility, effectiveness with small sample sizes, and ability to model strength and failure rates.

The relationship between the strain rate and microfibril angle (α) of CPGF is given in Eq. (4).

$$\text{Strain rate} = \ln\left(1 + \frac{\text{Change in length of the CPGF in mm}}{50\ \text{mm}}\right) = -\ln(\cos\alpha) \quad (4)$$

3. Results and discussion

3.1 Diameter and density of CPGF

Fig. 2 depicts a sample of an optical microscopic image of CPGF. The mean diameter and mean deviation of the CPGF were 607 and 27 μm, respectively. The summary of the comparison of chemical compositions, diameters and densities of CPGF and other similar plant fibers is presented in Table 1.

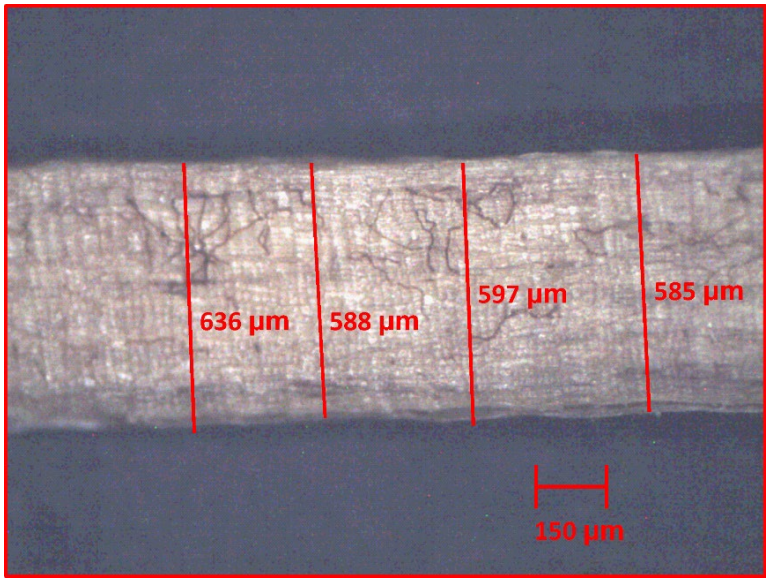

Fig. 2. Sample of optical microscopic image of CPGF.

270 **Table 1.** Comparison of chemical compositions, diameters and densities of CPGF with other similar plant fibers.

Fiber types	Physical properties		Chemical properties						References
	Density (kg/m^3)	Diameter (μm)	Cellulose (Wt.%)	Hemicellulose (Wt.%)	Lignin (Wt.%)	Wax (Wt.%)	Moisture content (Wt.%)	Ash (Wt.%)	
CPGF	1158.00±52	607.00±27	65.21±5.31	16.47±3.26	11.21±3.45	0.36±0.16	8.5±2.5	6.43±2.66	*Present study*
Ziziphus nummularia	1322	209.06±11.00	52.34	18.64	13.43	0.63	10.45	12.34	(Gurupranes et al. 2022)
Aerial roots banyan	1234	0.09-0.14	67.32	13.46	15.62	0.81	10.21	3.96	(Ganapathy et al. 2019)
Cattail	618.00±105.50	37.50±10.80	22.40±0.70	21.80±0.50	20.60±0.50	11.50±0.10	8.60±0.10	4.50±0.10	(Wu et al. 2021)
Derris scandens stem	1430.00±18.00	158.00-169.00	63.30	11.60	15.30	0.81	6.02	4.57	(Perumal and Sarala 2020)
Symphorema involucratum stem	1389	542.00	57.32	12.47	13.85	0.56	9.11	----	(Raju et al. 2021)
Cocconia grandis.L	1243	27.33	62.35	13.42	15.61	0.79	5.60	4.39	(Senthamaraikannan and Kathiresan 2018b)

Cissus quadrangularis root	1510	610.00-725.00	77.17	11.02	10.45	0.14	7.30	----	(Indran et al. 2016)
Tridax procumbens	1348	233.10	32.00	6.80	3.00	----	11.20	----	(Vijay et al. 2019)
Rosa hybrida bark	1194	214.00–238.00	52.99	18.49	17.34	----	11.60	----	(Shibly et al. 2024)
Buxus sempervirens	1326	30.74±0.69	51.78	18.42	17.36	0.49	14.31	16.44	(Rathinavelu and Paramathma 2022)
Mucuna atropurpurea	1082.00±29.00	289±21	58.74±5.74	16.31±3.21	14.22±3.36	0.38±0.08	11.12±2.11	7.66±2.49	(Senthamaraikannan and Saravanakumar 2022)
Ventilago maderaspatana	1236.00±18.42	89.27 ± 6.18	56.12±5.42	14.36±3.56	12.11± 3.28	0.42±0.16	8.89±2.66	9.46±1.04	(Rathinavelu et al. 2022)
Arial root *Ficus amplissima*	1340	27.93	52.64	10.64	13.72	0.44	8.68	10.75	(Ramesh Babu and Rameshkannan 2022a)
Ficus religiosa	25.62	1246	55.58	13.86	10.13	0.72	9.33	4.86	(Moshi et al. 2020a)
Cissus vitiginea stem	1287	355.74 ± 16.43	65.43	14.61	10.43	0.39	8.47	12.05	(Chakravarthy et al. 2020)

Grewia flavescens	1156	29.77±2.81	58.46	15.32	12.51	0.86	9.42	5.12	(Tiwari and Sarangi 2022)
Prosopis juliflora bark	580	20	61.65	16.14	17.11	0.61	9.48	5.20	(Saravanakumar et al. 2013)
Mariscus ligularis	768.59	243.60	26.20-58.32	19.10-25.85	9.50-10.74	0.73	14.46	11.74	(Garriba and Siddhi Jailani 2023)
Typha angustata	1015	105.00±10.15	73.54	10.11	6.23	0.23	6.56	2.54	(Manimaran et al. 2022)
Calotropis gigantea fruit bunch	457	----	64.47	9.64	13.56	1.93	7.27	3.13	(Ramasamy et al. 2018)
Echinochloa frumentacea leaf	896.00 ±32.14	493.09±10.33	60.31	9.30	10.11	0.36	8.04	10.14	(Rathinavelu and Paramathma 2022)
Cymbopogon nardus leaf	1305	115.10 ± 9.093	65.42	12.16	16.16	0.62	8.96	6.42	(Durgamalathi et al. 2024)
Hibiscus canescens stem	1425	447.60 ± 7.608	68.46	14.36	12.48	0.28	10.44	5.34	(Pradhan et al. 2023)

271

The diameter of CPGF was relatively lower when compared with other similar plant fibers, such as *Symphorema involucratum* stem (542 µm), *Cissus vitiginea* stem (355.74 ± 16.43 µm) and *Echinochloa frumentacea* leaf fiber (493.09±10.33 µm) (Mohan et al. 2022b). The density of the plant fiber is connected with the low weight and high strength ratio of composite materials. Fiber with lower density is preferable for composite fabrication. The density of the CPGF was 1158.00±52 kg/m³. The densities of many similar plant fibers are higher (Table 1), including *Cymbopogon nardus* leaf (1305 kg/m³), *Ventilago maderaspatana* (1236±18.42 kg/m³), and *Cissus quadrangularis* root (1510 kg/m³), as earlier reported (Malathi et al. 2023).

3.2 Chemical constitutions of CPGF

The chemical composition of plant fiber is an important parameter that influences its various properties. The higher cellulose content in the plant fiber is expected, since it provides improved thermal stability and tensile properties to the fibers. Cellulose in the CPGF was 65.21±5.31 wt.%. Several similar plant fibers, such as *Symphorema involucratum* stem of 57.32 wt.%, *Mariscus ligularis* of 26.20-58.32 wt.%, *Grewia flavescens* of 58.46 wt.% and *Rosa hybrida* bark fibers of 52.99 wt.% (Tiwari and Sarangi 2022; Garriba and Siddhi Jailani 2023) contained lower cellulose content than the CPGF. Higher hemicellulose content in the fiber is not welcomed, because it is a non-crystalline fraction. 16.47±3.26 wt.% of hemicellulose in the CPGF was quantified. Hemicellulose fractions of *Ziziphus nummularia* fiber (18.64 wt.%), Cattail fiber (21.8 ± 0.5 wt.%) and *Mariscus ligularis* fiber (19.10-25.85 wt.%) (Gurupranes et al. 2022; Garriba and Siddhi Jailani 2023) are higher than that of CPGF. Lignin in the plant prevents the plant from bacterial and fungal infections. However, fiber with higher lignin content is not a desirable reinforcement in polymer matrices. Lignin content of CPGF was 11.21±3.45 wt.%. In general, all plant fibers contain a small amount of wax. Fiber wax content acts as an oil and disrupts the interaction of the fiber with the matrix. A wax content of

0.36±0.16 wt.% was obtained from the CPGF. The calculated moisture content of the CPGF was 8.5±2.5 wt.%. A significant quantity of moisture was present in some cellulosic fibers, including fibers derived from aerial roots banyan (10.21 wt.%), *Mucuna atropurpurea* (11.12±2.11 wt.%) and *Hibiscus canescens* stem *(*10.44 wt.%) (Pradhan et al. 2023; Senthamaraikannan and Saravanakumar 2023). Ash content of 6.43±2.66 wt.% was present in the CPGF.

3.3 Crystallographic study of CPGF

The XRD spectrum of CPGF is depicted in Fig. 3. There are three significant peaks in Fig. 3 at 2θ = 14.89º, 16.53º and 22.67º. The cellulose diffraction pattern was observed to align with the diffraction pattern of cellulose Iβ (ICDD PDF Card No.: 00-056-1718) (Vinod et al. 2023; Srisuk et al. 2023) . The initial peak at 2θ (14.89º) corresponded to the lattice plane (1 -1 0), and the peak at 2θ (16.52º) corresponded to the lattice plane (1 1 0) (French and Santiago Cintrón 2013). The next diffraction peak at 2θ (22.67º) corresponded to the lattice plane (2 0 0) (French 2014). These intensity peaks correspond to the presence of Cellulose Iβ, which is a type of plant cellulose. The intensity for the 200 peak and the value of Iam determine the CI value. The CI value of CPGF was 67.84%. The CS of plant fiber is connected with the water-uptaking behavior of the fiber. CPGF exhibited a moderate CS value of 2.71 nm. CS values of various plant fibers, namely; *Ficus religiosa* (5.18 nm), *Mucuna atropurpurea* (2.75 nm) and aerial roots banyan (6.28 nm) have been reported (Moshi et al. 2020a). Importantly, the tensile, thermal and crystalline properties of CPGF and various biofibers are further presented in Table 2.

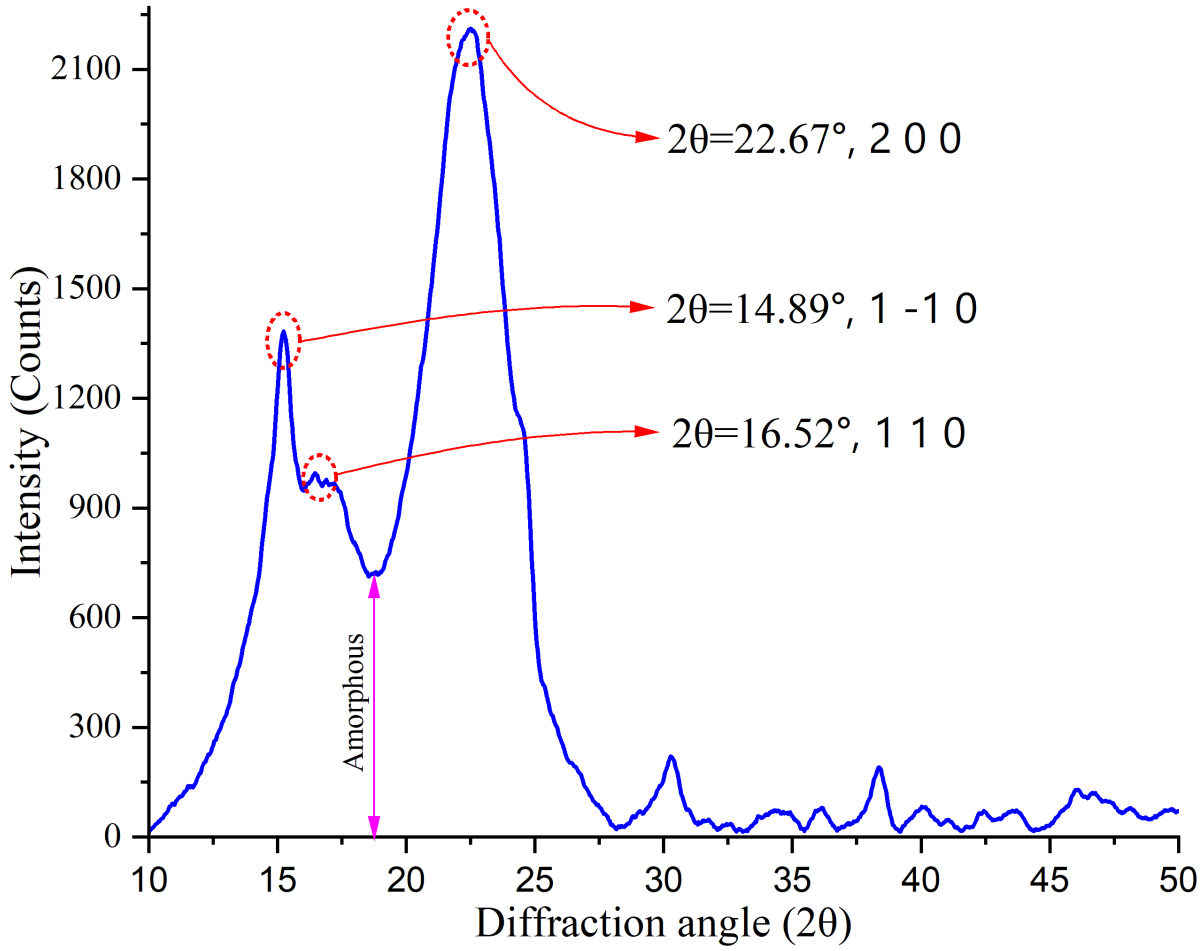

320

321 **Fig. 3.** XRD spectrum of CPGF.

322 **Table 2.** Comparison of tensile, thermal and crystalline characteristics of CPGF with other similar cellulosic plant fibers.

Fiber type	Thermal properties		Crystalline properties		Tensile properties			References
	Thermal stability (°C)	Maximum degradation temperature (°C)	CI (%)	CS (nm)	Tensile strength (MPa)	Tensile modulus (GPa)	Strain rate (%)	
CPGF	250	335	67.84	2.71	424.40±24.45	3.48±0.17	5.62±0.87	*Present study*
Cymbopogon nardus root fibers	200	368	59.16	2.13	-	-	-	(Sanjeevi et al. 2024)
Yucca aloifolia L. leaf fiber	193	357.7	69.43	2.46	801 ± 587	39 ± 28	2 ± 0.5	(do Nascimento et al. 2021)
Mariscus ligularis	258	314	72.33	3.15	109.00–134.00	3.27–5.06	3.32–9.13	(Garriba and Siddhi Jailani 2023)
Typha angustata	200	299	65.16	6.40	665.00±7.00	27.45±3.00	3.12±0.50	(Manimaran et al. 2022)
Cymbopogon nardus leaf fiber	200	326	49.69	4.32	435.90±16.05	55.25±6.10	1.33±0.24	(Durgamalathi et al. 2024)

Ziziphus nummularia	240	348	-	-	247.30±14.09	10.21±1.29	1.54 ±0.43	(Gurupranes et al. 2022)
Aerial roots banyan	230	358	-	-	247.30±14.09	10.21±1.29	1.54±0.43	(Ganapathy et al. 2019)
Cissus quadrangularis root	230	329	-	-	1857.00- 5330.00	68-203	3.57-8.37	(Indran et al. 2016)
Rosa hybrida bark	290	359	-	-	352.01	6.57	1.84	(Shibly et al. 2024)
Ficus religiosa	325	400	-	-	440.29±28.00	5.24±1.36	8.74±1.50	(Moshi et al. 2020a)

323

3.4 Chemical functional groups in CPGF

Fig. 4 shows the FTIR spectrum of CPGF. Wavenumbers in Fig. 4 indicate significant peaks. The first peak at 3273 cm^{-1} was linked to O–H stretching (cellulose) in the CPGF (Siva et al. 2020). A small peak established at 2921 cm^{-1} was typical C–H stretching (cellulose) of the fiber (Fu and Netravali 2020). A tiny peak observed at 2336 cm^{-1} was associated with wax content of the fiber (C≡C stretching) (Moshi et al. 2020b). The hemicellulose (C=O stretching) fraction in the CPGF was confirmed through a sharp peak existing at 1615 cm^{-1} (Rantheesh et al. 2023). The authorization of OH bending vibration of cellulose in the fiber was indicated by a moderate peak at 1323 cm^{-1} (Vinod et al. 2020). The C–OH stretching in the CPGF was identified by an additional sharp peak at 1017 cm^{-1}. The peak accredited beta glycosidic linkages in the CPGF at 784 cm^{-1} (Dalmis et al. 2020). The final peak recognized C-S stretching in the fiber at 654 cm^{-1} (Rathinavelu and Paramathma 2023). Important constitutions and linked functional groups in the CPGF are summarized in Table 3.

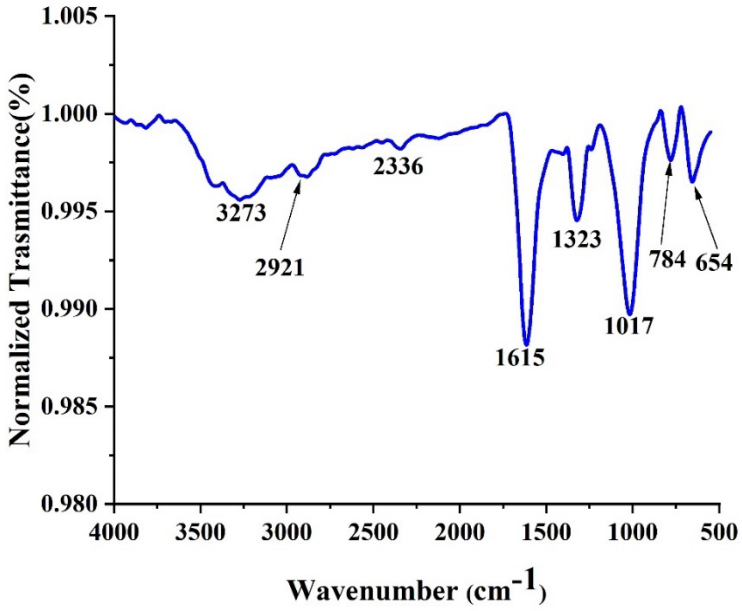

Fig. 4. FTIR spectrum of CPGF.

341 **Table 3.** Important constitutions and linked functional groups in the CPGF.

Stretching location (wavenumber, cm^{-1})	Chemical constitutions	Linked functional group	References
654	----	C-S stretching	(Rathinavelu and Paramathma 2023)
784	----	beta glycosidic linkages	(Dalmis et al. 2020)
1017	Lignin	C–OH stretching	(Dalmis et al. 2020)
1323	Cellulose	OH bending	(Vinod et al. 2020)
1615	Hemicellulose	C=O stretching	(Rantheesh et al. 2023)
2336	Wax	C≡C stretching	(Moshi et al. 2020b)
2921	Cellulose	C–H stretching	(Fu and Netravali 2020)
3273	Cellulose	O–H stretching	(Siva et al. 2020)

342

343 *3.5 Thermal analysis*

344 *3.5.1 Thermogravimetric analysis*

345 The merged thermogravimetric (TG) and derivative thermogravimetric (DTG) curves of
346 CPGF are shown in Fig. 5. The blue and red curves indicate the TG and DTG results,
347 respectively. The TG curve of the fiber revealed that the weight of the fiber was reduced as the
348 temperature increased. The weight reduction occurred in three phases. The initial weight
349 reduction phase at room temperature to 250 ºC can be assigned to rejecting water content in
350 the CPGF (Stalin et al. 2021). A notable reduction in fiber weight was observed within a

temperature ranged from 250 to 350 ºC, which can be attributed to the degradation of both hemicellulose and cellulose fractions in the CPGF. The concurrent deterioration of cellulose and lignin within the CPGF was observed between 350 and 475 ºC (Vijay et al. 2019). There was no change in the fiber weight when the temperature ranged from 475 to 800 ºC. From the DTG curve, three significant peaks were observed at 74, 335 and 424 ºC. A peak at 74 ºC was attributed to the ejection of water from CPGF. The dominant peak at 335 ºC is called the cellulose degradation peak or maximum degradation peak, interlinked with eliminating cellulose fraction in the fiber (Narayanasamy et al. 2020). Different biofibers exhibited the same type of cellulose degradation peak, namely, *Typha angustata* at 299 ºC, *Calotropis gigantea* fruit bunch at 317 ºC, *Mariscus ligularis* at 314 ºC and *Tridax procumbens* at 330 ºC. (Garriba and Siddhi Jailani 2023). Lignin fraction degradation was associated with the peak at 424 ºC.

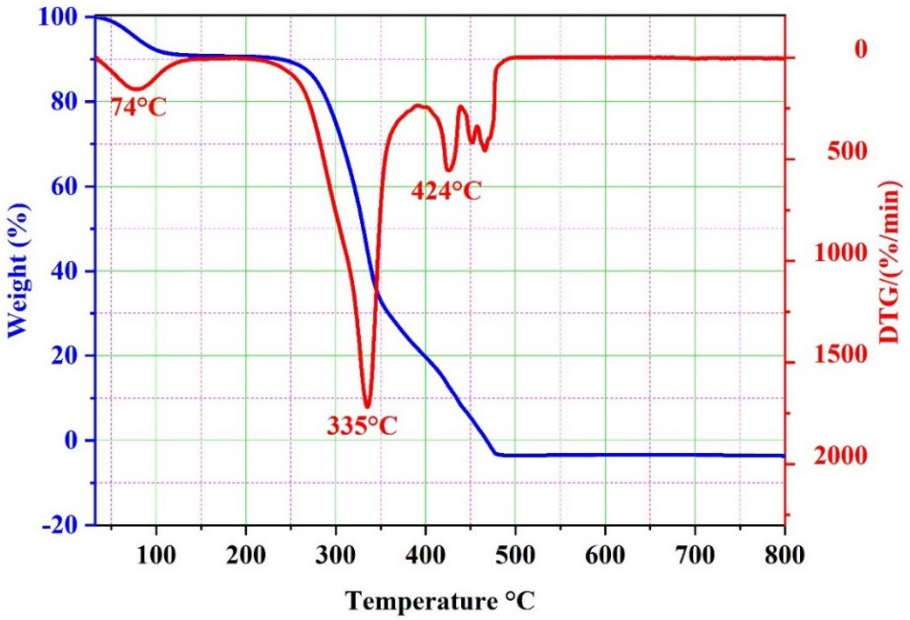

Fig. 5. Merged TG and DTG curves of CPGF.

3.5.2 Kinetic activation energy

The Broido profile of CPGF is depicted in Fig. 6. The estimated slope value of the Broido curve was -117115.72. The E_a value of cellulosic materials generally ranged from 60 to 150 kJ/mol (Belouadah et al. 2015). The E_a value of CPGF, computed as 97.40 kJ/mol, was significantly greater than that of previously reported fibers, such as *Ficus religiosa* of 68.02 kJ/mol, *Pennisetum glaucum* powder of 88.30 kJ/mol, *Albizia lebbeck* bark of 89.00 kJ/mol and *Acacia concinna* of 69.33 kJ/mol (Moshi et al. 2020a).

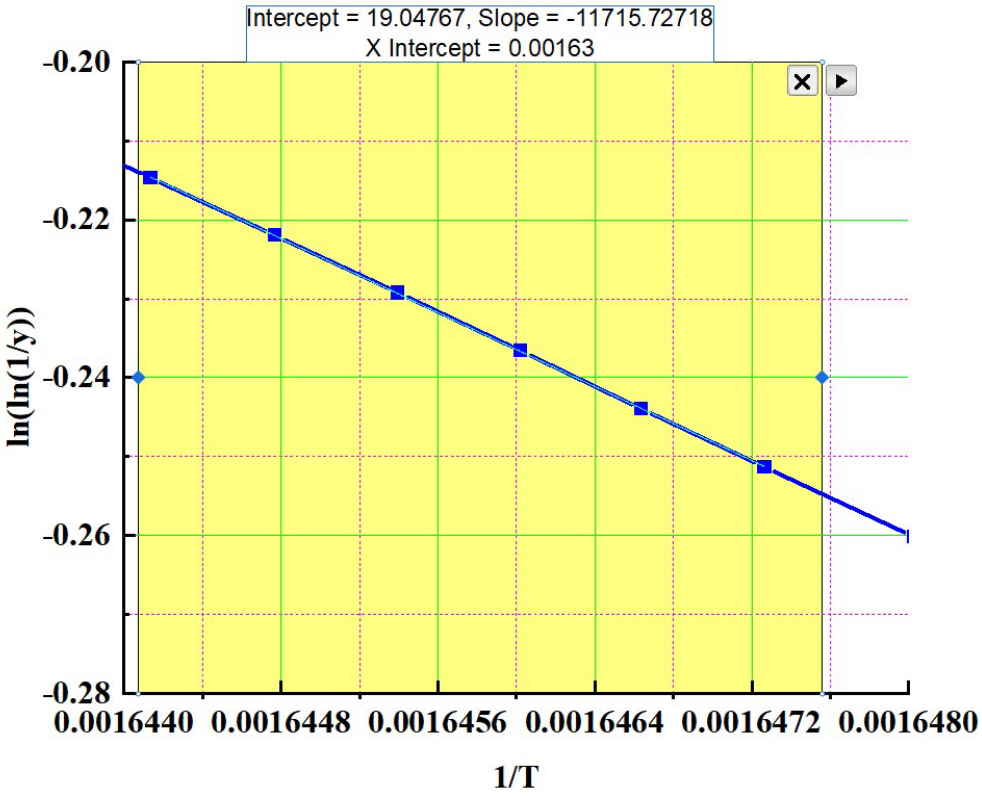

Fig. 6. Broido profile of CPGF.

3.5.3 Differential thermal analysis

Fig. 7 shows the DTA curve of CPGF, wherein three significant peaks were observed at 363, 433 and 471 ºC. Similar peaks were observed in the DTA curve of *Limonia acidissima* (wood apple) shell powder, *Trachelospermum jasminoides* fiber and Zea mays husk (Gedik 2021). Degradation of α-cellulose in the CPGF occurred at 363 ºC. Peaks observed at 433 and 471 ºC were attributed to the lignin in the CPGF.

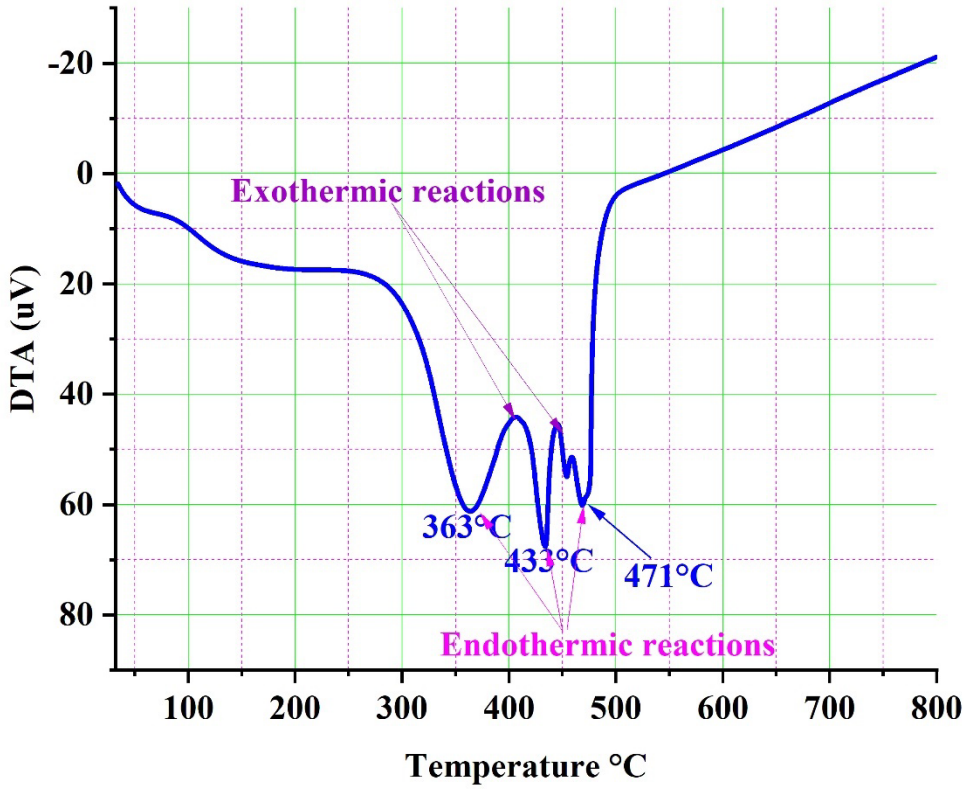

382

383 **Fig. 7.** DTA curve of CPGF.

384

385 *3.6 Surface investigation of CPGF*

386 *3.6.1 SEM analysis of CPGF*

387 Cross-sectional SEM images of CPGF captured at various magnifications of 250, 500, 1000
388 and 1500x are depicted in Fig. 8. The outer surface of the CPGF, as depicted in Figs 8(b) and
389 (d), was contaminated with wax and impurities. Microfibrils of the CPGF were observed in
390 Fig. 8(b). Wax, hemicellulose and impurities deposited on surface of the fiber contributed to
391 its smoothness. Reinforcing with smooth-surfaced fibers is not advised, due to reduced fiber-
392 matrix adhesion (Raju et al. 2021). The smooth surface of the CPGF is shown in Fig. 8(c).
393 However, a rough surface was observed in some spots of the fiber. Overall, a suitable fiber
394 surface treatment or modification is proposed, using chemical solutions, such as sodium

hydroxide, benzoyl peroxide and stearic acid, to enhance the roughness of the fiber (Durgamalathi et al. 2024).

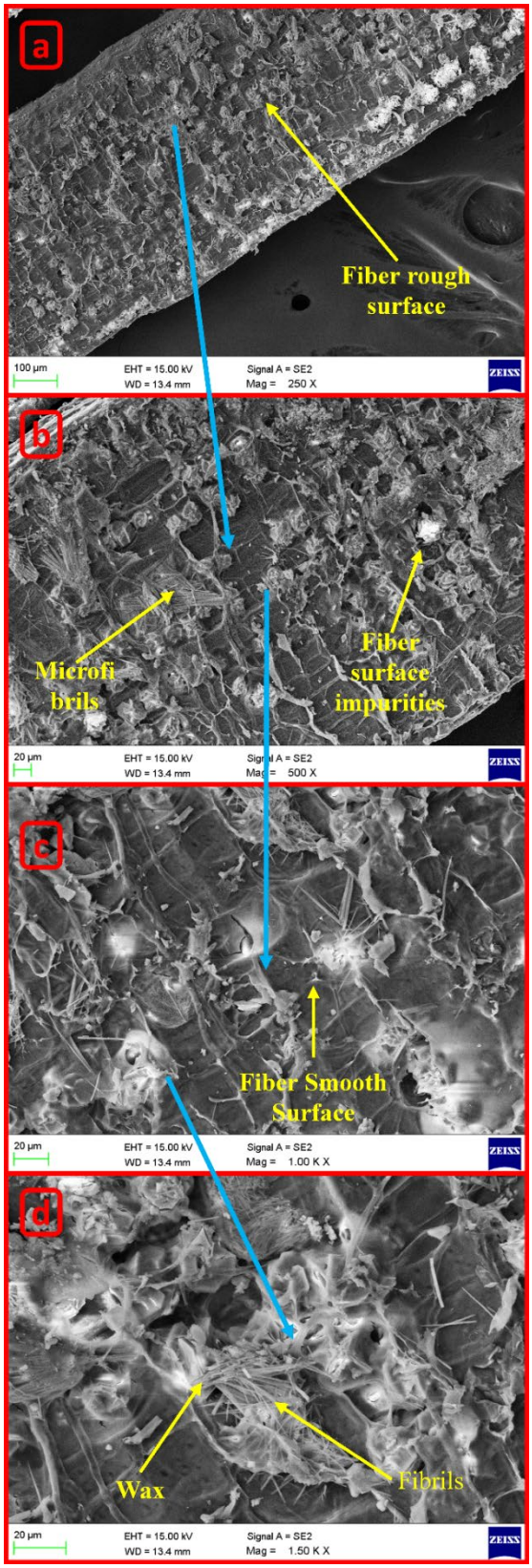

Fig. 8. Cross-sectional SEM images of CPGF at magnifications of (a) 250, (b) 500, (c) 1000 and (d) 1500x.

3.6.2 EDX analysis of CPGF

The outcomes of the EDX analysis of CPGF are shown in Fig. 9. All the biofibers contained carbon and oxygen elements, since they are associated with the cellulose and hemicellulose fractions of the fiber. All other elements in the EDX spectrum of fibers, except carbon (C) and oxygen (O), were contaminants (Tiwari and Sarangi 2022). A considerable quantity of calcium (Ca) element was spotted in the EDX spectrum of CPGF. *Grewia flavenscens* and *Mucuna atropurpurea* fibers also contained Ca (Senthamaraikannan and Saravanakumar 2022; Tiwari and Sarangi 2022). Another element in the CPGF was potassium (K), indicating an impurity. The EDX spectrum of *Ficus amplissima* aerial root and *Ziziphus nummularia* fibers possessed a small quantity of K (Gurupranes et al. 2022). Table 4 presents the quantities of distinct elements present on the surface of a variety of plant fibers in comparison with CPGF.

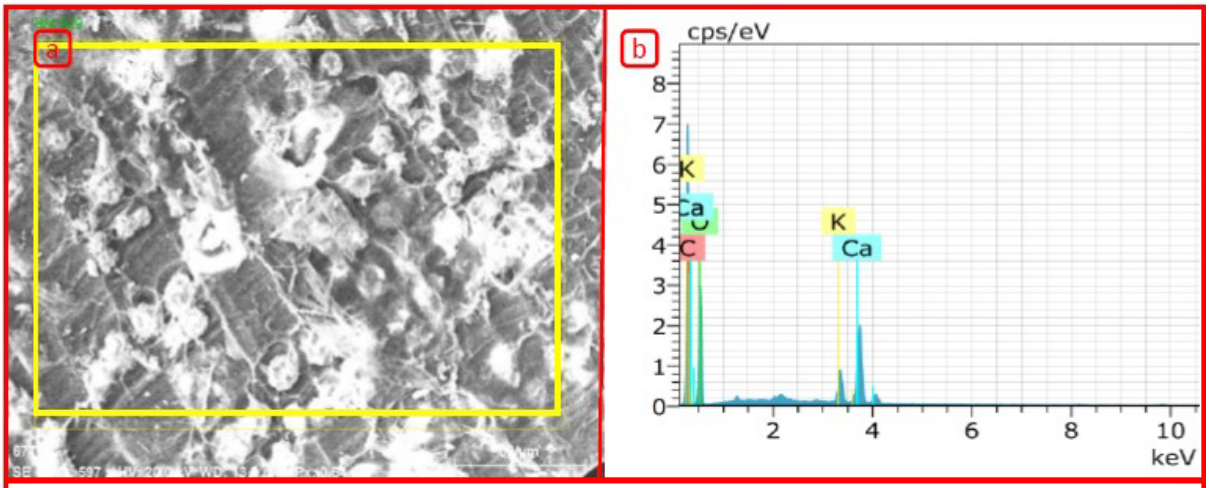

c

Elements		
	Weight (%)	Atomic (%)
C	47.75	57.33
O	44.06	39.71
Ca	6.34	2.28
K	1.86	0.68

412
413 **Fig. 9.** EDX analysis of CPGF.

Table 4. Comparison of elements present in EDX spectra of CPGF with other similar plant fibers (Senthamaraikannan and Saravanakumar 2022; Tiwari and Sarangi 2022; Gurupranes et al. 2022; Ramesh Babu and Rameshkannan 2022b; Durgamalathi et al. 2024).

Elements	CPGF (*present study*)		Other similar plant fibers									
			Ficus amplissima aerial root		*Ziziphus nummularia*		*Mucuna atropurpurea*		*Cymbopogon nardus* leaf		*Grewia flavenscens*	
	Weight (%)	Atomic (%)	Weight (%)	Atomic (%)	Weight (%)	Atomic (%)	Weight (%)	Atomic (%)	Weight (%)	Atomic (%)	Weight (%)	Atomic (%)
C	47.75	57.33	62.09	69.27	46.37	54.14	48.63	61.69	46.69	43.40	40.54	50.25
O	44.06	39.71	35.70	29.90	50.89	44.65	31.59	30.09	40.06	49.59	49.46	46.02
Ca	6.34	2.28	----	----	0.87	0.30	5.08	1.93	----	----	9.18	3.41
K	1.86	0.68	1.63	0.56	0.35	0.13	10.81	4.21	----	----	0.82	0.31
Al	----	----	0.04	0.02	0.47	0.24	0.49	0.27	----	----	----	----
Si	----	----	0.54	0.26	----	----	----	----	13.25	7.01	----	----
P	----	----	----	----	----	----	2.00	0.98	----	----	----	----
Cl	----	----	----	----	0.57	0.23	----	----	----	----	----	----
Mg	----	----	----	----	0.54	0.31	1.03	0.65	----	----	----	----
S	----	----	----	----	----	----	0.37	0.17	----	----	----	----

3.6.3 AFM analysis of CPGF

AFM micrographs of CPGF are depicted in Fig. 10. The AFM result of CPGF was compared with the other cellulosic fibers in Table 5. A higher average roughness (R_a) is an expected quality for a suitable reinforcement. The R_a value of CPGF was 7.549 nm and much smaller when compared with that of *Cyperus pangorei* fiber (625 nm), *Sida mysorensis* fiber (51.567 nm) and *Mucuna atropurpurea* fiber (27.113 nm). However, the R_a value of CPGF (7.549 nm) was higher than that of *Ficus racemosa* fiber (6.763 nm), *Carica papaya* bark fiber (2.433 nm) and *Areva javanica* fiber (0.693 nm) (Manimaran et al. 2019; Maran et al. 2020). The lower Ra value of CPGF suggested the presence of wax and impurities on its surface. The roughness skewness (R_{sk}) of CPGF was -1.784. The tiny holes on surface the fiber can be understood through the R_{sk} value, as negative R_{sk} established the small holes on the surface of CPGF.

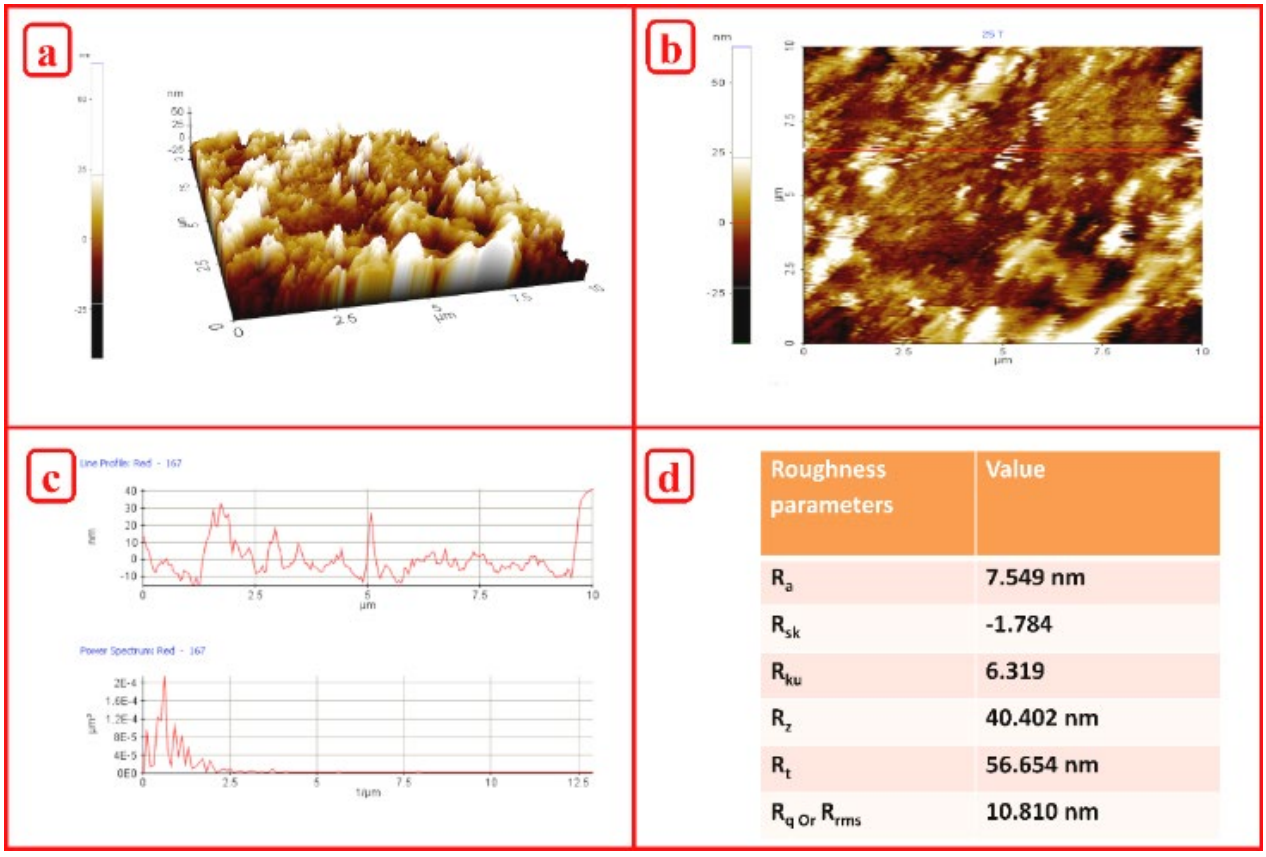

Fig. 10. AFM results of CPGF.

Table 5. Comparison of outcomes of AFM analysis of CPGF with other similar plant fibers.

Fiber type	Average roughness (R_a) (nm)	Roughness skewness (R_{sk})	Roughness kurtosis (R_{ku})	Ten-point average roughness (R_z) (nm)	Maximum peak-to-valley height (R_t) (nm)	Root mean square roughness (R_q or R_{rms}) (nm)	References
CPGF	7.549	-1.784	6.319	40.402	56.654	10.810	*Present study*
Cymbopogon nardus leaf	20.876	-2.009	8.195	99.111	175.569	30.117	(Durgamalathi et al. 2024)
Mucuna atropurpurea	27.113	-1.747	6.318	185.604	207.532	39.620	(Senthamaraikannan and Saravanakumar 2022)
Acacia concinna	11.217	-0.507	3.473	60.083	82.608	14.808	(Amutha and Senthilkumar 2021)
Aerial roots banyan	2.946	-3.217	14.891	24.320	33.662	4.970	(Ganapathy et al. 2019)

Cyperus pangorei	625.000	-1.740	11.000	547.000	104.000	918.000	(Rajini et al. 2021)
Ficus racemosa	6.763	-0.442	2.521	29.226	39.504	8.231	(Manimaran et al. 2019)
Derris scandens stem	105.959	−0.251	1.400	721.366	1446.490	138.866	(Perumal and Sarala 2020)
Grewia monticola sond	10.425	-0.594	4.733	59.793	87.258	13.647	(Almeshaal et al. 2022)
Areva javanica	0.693	0.067	3.108	4.257	5.295	0.877	(Ahmed et al. 2019)
Pongamia pinnata L.	4.880	-1.350	5.100	29.460	35.330	6.502	(Umashankaran and Gopalakrishnan 2021)
Ventilago maderaspatana	28.000	1.240	4.363	151.000	158.000	38.000	(Rathinavelu et al. 2022)
Perotis indica	9.456	-0.996	4.154	56.730	72.381	12.544	(Prithiviraj et al. 2016)

Furcraea foetida	18.005	−0.326	2.332	77.201	93.845	21.756	(Manimaran et al. 2018)
Aristida adscensionis	12.700	−0.076	3.349	----	----	----	(Manimaran et al. 2020)
Phaseolus vulgaris	5.000	-1.584	6.347	33.000	40.000	7.000	(Babu et al. 2022)
Carica papaya bark	2.433	-1.923	9.095	20.014	27.715	3.887	(Saravanakumaar et al. 2018)
Senna auriculata	75.997	-0.032	0.181	384.011	793.165	96.471	(Ganesh et al. 2019)
Water hyacinth	151.000	-0.125	1.606	310.000	----	----	(Sumrith et al. 2020)

The R_{ku} of CPGF was 6.319. The surface of CPGF was considered smooth, since the R_{ku} of CPGF was greater than 3.000 (Gokulkumar et al. 2023). The R_{ku} values of many raw plant fibers, such as aerial roots banyan (14.891), *Pongamia pinnata L*. (5.100) and *Grewia monticola* sond (4.733), are greater than 3.000. However, *Derris scandens* stem fiber (1.400), *Furcraea foetida* fiber (2.332) and *Senna auriculata* fiber (0.181) have lower R_{ku} values (Manimaran et al. 2018; Almeshaal et al. 2022).

3.7 Mechanical testing of CPGF

The tensile properties of a single fiber significantly impact the mechanical characteristics of plastics reinforced with fiber. The single fiber tensile strength of CPGF was 424.40±24.45 MPa. The tensile strengths of *Cocconia grandis.L* fiber (273.00±27.74 MPa), *Rosa hybrida* bark fiber (352.01 MPa), *Cissus vitiginea* stem fiber (315.47±38.00 MPa) and *Grewia flavescens* fiber (276.90±25.43 MPa) are considerably lower than that of CPGF (Shibly et al. 2024). The Young's modulus of CPGF was 3.48±0.17 GPa. Nearly the same Young's modulus values have been obtained in *Mariscus ligularis* fiber (3.27–5.06 GPa) and *Mucuna atropurpurea* fiber (2.88±1.03 GPa). The strain rate and microfibril angle of fiber are directly proposal as per equation 4 (Senthamaraikannan and Saravanakumar 2022). The strain rate and microfibril angle of CPGF were 5.62±0.87% and 18.97±1.48º, respectively. Variations in diameter and other plant parameters induce fluctuations in the mechanical properties of plant fibers. The results of the statistical testing of the diameter and single fiber tensile properties of CPGF are depicted in Fig. 11. Weibull analysis is a suitable method for statistical verification. The results of the Weibull analysis established the suitability of CPGF as a natural reinforcement, because each parameter was precisely situated within the limit of the Weibull curve (Tiwari and Sarangi 2022).

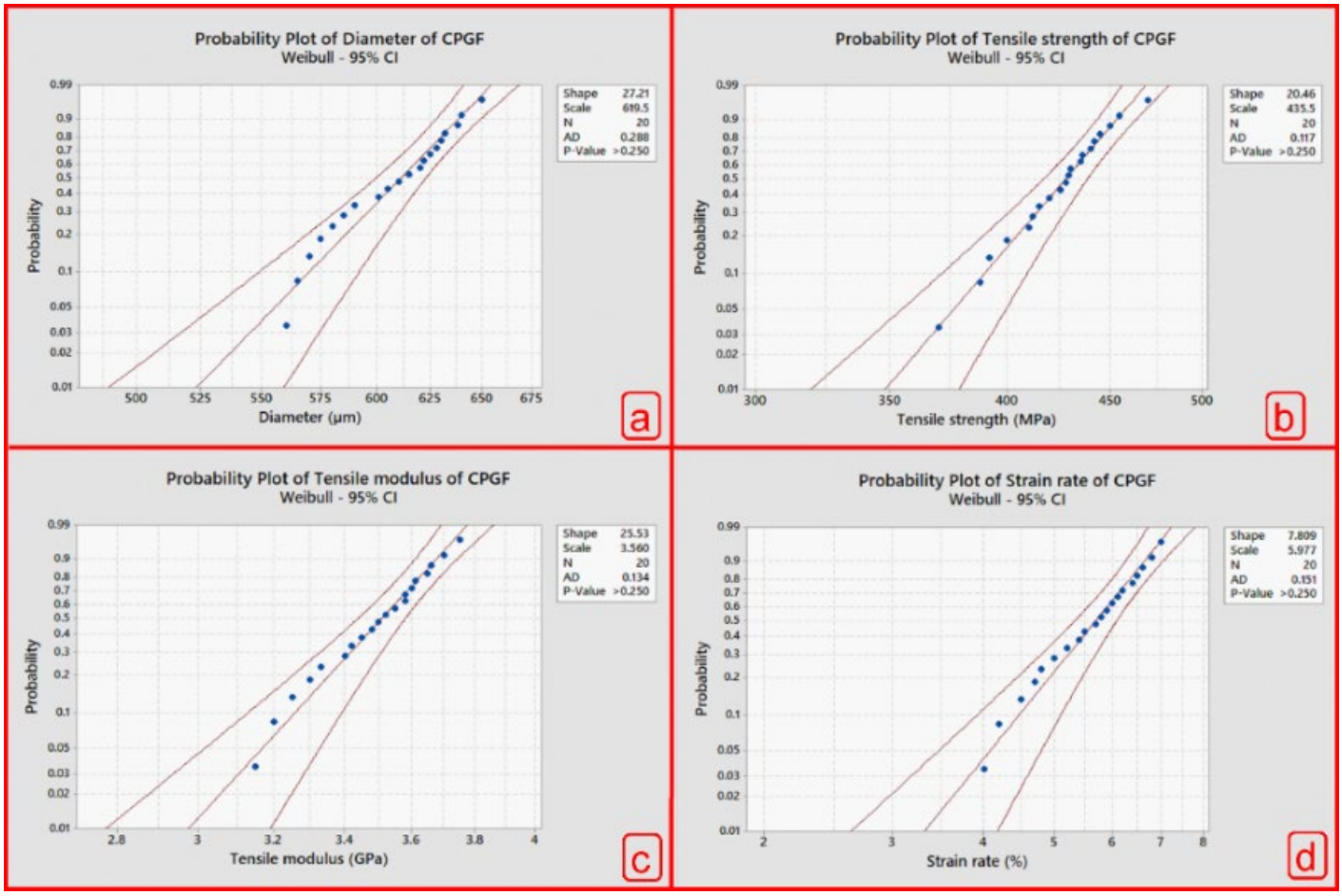

462 **Fig. 11.** Statistical testing of diameter and single fiber tensile properties of CPGF.

463

464 **4. Conclusions**

465 The extraction and characterization of CPGF as a potential reinforcement in PMCs have
466 been investigated. The extracted CPGF had a diameter and density of 607±27 µm and
467 1158.00±52 kg/m^3, respectively. Its higher cellulose content of 65.21±5.31 wt.% and CI of
468 67.84% were significant properties associated with improved thermal and tensile properties.
469 TGA curve inferred that around 10 wt.% of fiber only degraded at 250 ºC. CPGF exhibited a
470 maximum degradation temperature of 335 ºC and an E_a of 97.4 kJ/mol. Unwanted elements,
471 including Ca and K in the EDX spectrum of CPGF, indicated impurities in its outer profile. The
472 smooth surface of the fiber was observed from its SEM images. In addition, the results obtained
473 from AFM analysis agreed with the SEM micrographs.

Using a single fiber tensile testing machine, CPGF exhibited tensile strength of 424.40±24.45 MPa and modulus of 3.480±0.1696 GPa. Tensile testing results were statistically verified through Weibull analysis with the help of Minitab 18 software. Summarily, based on the results obtained from this innovative study, the possibility of using CPGF-reinforced plastics in a wide range of potential applications across many industries, including automotive, building/construction, paper and furniture as well as lightweight composite equipment in sports, apparel and biodegradable materials in packaging. However, a suitable fiber surface modification or treatment is proposed to induce a rougher surface on the fiber, as required for an enhanced fiber-matrix interfacial adhesion, consequent properties and performances of its potential PMCs.

Declarations

Ethical Approval

Not applicable

Competing interests

The author(s) declared no potential conflicts of interest concerning this article's research, authorship and publication.

Authors' contributions

P. Senthamaraikannan: Investigation, formal analysis, visualization, writing original draft; **S. Indran**: Methodology, manuscript editing and review; **S. S. Saravanakumar**: Methodology, and review; **Sikiru O. Ismail**: Manuscript writing, editing and review; **Suchart Siengchin**: Methodology, manuscript editing and review

Funding

The author(s) received no financial support for this article's research, authorship, and/or publication.

Availability of data and materials

No dataset has been provided for this submission.

Acknowledgements

The authors gratefully acknowledge the support of Dr. S. Karuppusamy, Department of Botany, Madura College, Madurai, Tamil Nadu.

References

Ahmed MJ, Balaji MAS, Saravanakumar SS, et al (2019) Characterization of Areva javanica fiber – A possible replacement for synthetic acrylic fiber in the disc brake pad. J Ind Text 49:294–317. https://doi.org/10.1177/1528083718779446

Almeshaal M, Palanisamy S, Murugesan TMTM, et al (2022) Physico-chemical characterization of Grewia Monticola Sond (GMS) fibers for prospective application in biocomposites. J Nat Fibers 00:1–15. https://doi.org/10.1080/15440478.2022.2123076

Amutha V, Senthilkumar B (2021) Physical, Chemical, Thermal, and Surface Morphological Properties of the Bark Fiber Extracted from Acacia Concinna Plant. J Nat Fibers 18:1661–1674. https://doi.org/10.1080/15440478.2019.1697986

Arul Marcel Moshi A, Ravindran D, Sundara Bharathi SRR, et al (2020) Characterization of natural cellulosic fiber extracted from Grewia damine flowering plant's stem. Int J Biol Macromol 164:1246–1255. https://doi.org/10.1016/j.ijbiomac.2020.07.225

523 Babu BG, Princewinston D, Saravanakumar SS, et al (2022) Investigation on the
524 Physicochemical and Mechanical Properties of Novel Alkali-treated Phaseolus vulgaris
525 Fibers. J Nat Fibers 19:770–781. https://doi.org/10.1080/15440478.2020.1761930

526 Belouadah Z, Ati A, Rokbi M (2015) Characterization of new natural cellulosic fiber from
527 Lygeum spartum L. Carbohydr Polym 134:429–437.
528 https://doi.org/10.1016/j.carbpol.2015.08.024

529 Belouadah Z, Toubal L, Belhaneche-Bensemra N, Ati A (2021) Characterization of ligno-
530 cellulosic fiber extracted from Atriplex halimus L. plant. Int J Biol Macromol 168:806–
531 815. https://doi.org/10.1016/j.ijbiomac.2020.11.142

532 Bharath KNN, Madhu P, Gowda TGYGYY, et al (2020) Alkaline Effect on Characterization
533 of Discarded Waste of Moringa oleifera Fiber as a Potential Eco-friendly Reinforcement
534 for Biocomposites. J Polym Environ 28:2823–2836. https://doi.org/10.1007/s10924-
535 020-01818-4

536 Binoj JS, Raj RE, Daniel BSS, Saravanakumar SS (2016) Optimization of short Indian Areca
537 fruit husk fiber (Areca catechu L.)–reinforced polymer composites for maximizing
538 mechanical properties. Int J Polym Anal Charact 21:112–122.
539 https://doi.org/10.1080/1023666X.2016.1110765

540 Boominathan S, Suyambulingam I, Narayanaperumal S, et al (2023) Comprehensive
541 characterization of novel bioplasticizer from Pandanus tectorius leaves: a sustainable
542 biomaterial for biofilm applications. Macromol Res 31:1061–1075.
543 https://doi.org/10.1007/s13233-023-00192-z

544 Broido A (1969) A simple, sensitive graphical method of treating thermogravimetric analysis
545 data. J Polym Sci Part A-2 Polym Phys 7:1761–1773.
546 https://doi.org/10.1002/pol.1969.160071012

547 Chakravarthy S, S M, Raju JSN, Md JS (2020) Characterization of novel natural cellulosic
548 fiber extracted from the stem of Cissus vitiginea plant. Int J Biol Macromol 161:1358–
549 1370. https://doi.org/10.1016/j.ijbiomac.2020.07.230

550 Conrad CM (1944) Determination of Wax in Cotton Fiber a New Alcohol Extraction Method.
551 Ind Eng Chem - Anal Ed 16:745–748. https://doi.org/10.1021/i560136a007

552 Dalmis R, Köktaş S, Seki Y, Kılınç AÇ (2020) Characterization of a new natural cellulose
553 based fiber from Hierochloe Odarata. Cellulose 27:127–139.
554 https://doi.org/10.1007/s10570-019-02779-1

555 do Nascimento HM, dos Santos A, Duarte VA, et al (2021) Characterization of natural
556 cellulosic fibers from Yucca aloifolia L. leaf as potential reinforcement of polymer
557 composites. Cellulose 28:5477–5492. https://doi.org/10.1007/s10570-021-03866-y

558 Durgamalathi P, Pulikkal AK, Ramesan MT, Nagarajan S (2024) Mercerized Cymbopogon
559 nardus shoot fiber as reinforcing filler. Mater Chem Phys 313:128739.
560 https://doi.org/10.1016/j.matchemphys.2023.128739

561 Felix Sahayaraj A, Muthukrishnan M, Ramesh M (2022) Experimental investigation on
562 physical, mechanical, and thermal properties of jute and hemp fibers reinforced hybrid
563 polylactic acid composites. Polym Compos 43:2854–2863.
564 https://doi.org/10.1002/pc.26581

565 French AD, Santiago Cintrón M (2013) Cellulose polymorphy, crystallite size, and the Segal
566 Crystallinity Index. Cellulose 20:583–588. https://doi.org/10.1007/s10570-012-9833-y

567 Fu D, Netravali AN (2020) Green composites based on avocado seed starch and nano- and
568 micro-scale cellulose. Polym Compos 41:4631–4648. https://doi.org/10.1002/pc.25739

569 Ganapathy T, Sathiskumar R, Senthamaraikannan P, et al (2019) Characterization of raw and

570 alkali treated new natural cellulosic fibres extracted from the aerial roots of banyan tree.
571 Int J Biol Macromol 138:573–581. https://doi.org/10.1016/j.ijbiomac.2019.07.136

572 Garriba S, Siddhi Jailani H (2023) Extraction and characterization of natural cellulosic fiber
573 from Mariscus ligularis plant as potential reinforcement in composites. Int J Biol
574 Macromol 253:127609. https://doi.org/10.1016/j.ijbiomac.2023.127609

575 Gedik G (2021) Extraction of new natural cellulosic fiber from Trachelospermum
576 jasminoides (star jasmine) and its characterization for textile and composite uses.
577 Cellulose 28:6899–6915. https://doi.org/10.1007/s10570-021-03952-1

578 Gokulkumar S, Suyambulingam I, Divakaran D, et al (2023) Facile exfoliation and
579 physicochemical characterization of biomass-based cellulose derived from Lantana
580 aculeata leaves for sustainable environment. Macromol Res 31:1163–1178.
581 https://doi.org/10.1007/s13233-023-00197-8

582 Gurupranes, I R, N SS (2022) Suitability assessment of raw-alkalized Ziziphus nummularia
583 bark fibers and its polymeric composites for lightweight applications. Polym Compos
584 43:5059–5075. https://doi.org/10.1002/pc.26782

585 Ilaiya Perumal., C Sarala. R (2020) Characterization of a new natural cellulosic fiber
586 extracted from Derris scandens stem. Int J Biol Macromol 165:2303–2313.
587 https://doi.org/10.1016/j.ijbiomac.2020.10.086

588 Indran S, Raj REE, Daniel BSSSS, Saravanakumar SSS (2016) Cellulose powder treatment
589 on Cissus quadrangularis stem fiber-reinforcement in unsaturated polyester matrix
590 composites. J Reinf Plast Compos 35:212–227.
591 https://doi.org/10.1177/0731684415611756

592 Jaiswal D, Devnani GLL, Rajeshkumar G, et al (2022) Review on extraction,

593 characterization, surface treatment and thermal degradation analysis of new cellulosic
594 fibers as sustainable reinforcement in polymer composites. Curr Res Green Sustain
595 Chem 5:100271. https://doi.org/10.1016/j.crgsc.2022.100271

596 Kumar S, Saha A (2024) Utilization of coconut shell biomass residue to develop sustainable
597 biocomposites and characterize the physical, mechanical, thermal, and water absorption
598 properties. Biomass Convers Biorefinery 14:12815–12831.
599 https://doi.org/10.1007/s13399-022-03293-4

600 Kumar S, Saha A, Bhowmik S (2022) Accelerated weathering effects on mechanical, thermal
601 and viscoelastic properties of kenaf/pineapple biocomposite laminates for load bearing
602 structural applications. J Appl Polym Sci 139:. https://doi.org/10.1002/app.51465

603 Kurschner K and Hoffer A (1933) Cellulose and cellulose derivative. Fresenius' J Anal Chem
604 92:145–154

605 Malathi D, Pulikkal AK, Ramesan MT, Nagarajan S (2023) Bio-fiber recovery from
606 industrially discarded shoot waste (Cymbopogon nardus): a comprehensive study for
607 reinforcement in sustainable composites. Biomass Convers Biorefinery.
608 https://doi.org/10.1007/s13399-023-04038-7

609 Manimaran P, Saravanan SP, Prithiviraj M (2019) Investigation of Physico Chemical
610 Properties and Characterization of New Natural Cellulosic Fibers from the Bark of Ficus
611 Racemosa. J Nat Fibers 0478: https://doi.org/10.1080/15440478.2019.1621233

612 Manimaran P, Saravanan SPP, Sanjay MRR, et al (2020) New Lignocellulosic Aristida
613 adscensionis Fibers as Novel Reinforcement for Composite Materials: Extraction,
614 Characterization and Weibull Distribution Analysis. J Polym Environ 28:803–811.
615 https://doi.org/10.1007/s10924-019-01640-7

616 Manimaran P, Senthamaraikannan P, Sanjay MRR, et al (2018) Study on characterization of
617 Furcraea foetida new natural fiber as composite reinforcement for lightweight
618 applications. Carbohydr Polym 181:650–658.
619 https://doi.org/10.1016/j.carbpol.2017.11.099

620 Manimaran P, Vignesh V, Khan A, et al (2022) Extraction and characterization of natural
621 lignocellulosic fibres from Typha angustata grass. Int J Biol Macromol 222:1840–1851.
622 https://doi.org/10.1016/j.ijbiomac.2022.09.273

623 Mansingh B, Joseph Selvi B, Abu Hassan S, et al (2021) Characterization of chemically
624 treated new natural cellulosic fibers from peduncle of Cocos nucifera L. Var typica.
625 Polym Compos 42:6403–6416. https://doi.org/10.1002/pc.26307

626 Maran M, Kumar R, Senthamaraikannan P, et al (2020) Suitability Evaluation of Sida
627 mysorensis Plant Fiber as Reinforcement in Polymer Composite. J Nat Fibers 1–11.
628 https://doi.org/10.1080/15440478.2020.1787920

629 Marichelvam MKK, Manimaran P, Verma A, et al (2021) A novel palm sheath and sugarcane
630 bagasse fiber based hybrid composites for automotive applications: An experimental
631 approach. Polym Compos 42:512–521. https://doi.org/10.1002/pc.25843

632 Michell AJ (1993) Second-derivative FTIR spectra of native celluloses from Valonia and
633 tunicin. Carbohydr Res 241:47–54. https://doi.org/10.1016/0008-6215(93)80093-T

634 Mohan SJ, Devasahayam PSS, Suyambulingam I, Siengchin S (2022a) Suitability
635 characterization of novel cellulosic plant fiber from Ficus benjamina L. aerial root for a
636 potential polymeric composite reinforcement. Polym Compos.
637 https://doi.org/10.1002/pc.27080

638 Mohan SJ, Devasahayam PSS, Suyambulingam I, Siengchin S (2022b) Suitability

639 characterization of novel cellulosic plant fiber from Ficus benjamina L. aerial root for a
640 potential polymeric composite reinforcement. Polym Compos 43:9012–9026.
641 https://doi.org/10.1002/pc.27080

642 Moshi AAM, Madasamy S, Bharathi SRS, et al (2019) Investigation on the mechanical
643 properties of sisal – Banana hybridized natural fiber composites with distinct weight
644 fractions. Int Conf Mater Manuf Mach 2019 2128:020029.
645 https://doi.org/10.1063/1.5117941

646 Moshi AM, D. R, S.R. SB, et al (2020) Characterization of surface-modified natural
647 cellulosic fiber extracted from the root of Ficus religiosa tree. Int J Biol Macromol
648 156:997–1006. https://doi.org/10.1016/j.ijbiomac.2020.04.117

649 NagarajaGanesh B, Ganeshan P, Ramshankar P, Raja K (2019) Assessment of natural
650 cellulosic fibers derived from Senna auriculata for making light weight industrial
651 biocomposites. Ind Crops Prod 139:111546.
652 https://doi.org/10.1016/j.indcrop.2019.111546

653 Narayana Perumal S, Suyambulingam I, Divakaran D, Siengchin S (2023) Extraction and
654 Physico-Mechanical and Thermal Characterization of a Novel Green Bio-Plasticizer
655 from Pedalium murex Plant Biomass for Biofilm Application. J Polym Environ
656 31:4353–4368. https://doi.org/10.1007/s10924-023-02898-8

657 Narayanasamy P, Balasundar P, Senthil S, et al (2020) Characterization of a novel natural
658 cellulosic fiber from Calotropis gigantea fruit bunch for ecofriendly polymer
659 composites. Int J Biol Macromol 150:793–801.
660 https://doi.org/10.1016/j.ijbiomac.2020.02.134

661 Pradhan R, Palai BK, Thatoi DN, et al (2023) Characterization of novel cellulosic fibers
662 extracted from Hibiscus canescens stem. Biomass Convers Biorefinery.

https://doi.org/10.1007/s13399-023-04645-4

Prithiviraj M, Muralikannan R, Senthamaraikannan P, Saravanakumar SSS (2016) Characterization of new natural cellulosic fiber from the Perotis indica plant. Int J Polym Anal Charact 21:669–674. https://doi.org/10.1080/1023666X.2016.1202466

Rajini N, Mayandi K, Manoj Prabhakar M, et al (2021) Tribological Properties of Cyperus Pangorei Fibre Reinforced Polyester Composites(Friction and Wear Behaviour of Cyperus Pangorei Fibre/Polyester Composites). J Nat Fibers 18:261–273. https://doi.org/10.1080/15440478.2019.1621232

Raju JSN, Depoures MV, Kumaran P (2021) Comprehensive characterization of raw and alkali (NaOH) treated natural fibers from Symphirema involucratum stem. Int J Biol Macromol 186:886–896. https://doi.org/10.1016/j.ijbiomac.2021.07.061

Ramasamy R, Obi Reddy K, Varada Rajulu A (2018) Extraction and Characterization of Calotropis gigantea Bast Fibers as Novel Reinforcement for Composites Materials. J Nat Fibers 15:527–538. https://doi.org/10.1080/15440478.2017.1349019

Ramesh Babu S, Rameshkannan G (2022a) Aerial Root Fibres of Ficus amplissima as a Possible Reinforcement in Fibre-Reinforced Plastics for Lightweight Applications: Physicochemical, Thermal, Crystallographic, and Surface Morphological Behaviours. J Nat Fibers 19:7909–7924. https://doi.org/10.1080/15440478.2021.1958422

Ramesh Babu S, Rameshkannan G (2022b) Aerial Root Fibres of Ficus amplissima as a Possible Reinforcement in Fibre-Reinforced Plastics for Lightweight Applications: Physicochemical, Thermal, Crystallographic, and Surface Morphological Behaviours. J Nat Fibers 19:7909–7924. https://doi.org/10.1080/15440478.2021.1958422

Rantheesh J, Indran S, Raja S, Siengchin S (2023) Isolation and characterization of novel

686 micro cellulose from Azadirachta indica A. Juss agro-industrial residual waste oil cake
687 for futuristic applications. Biomass Convers Biorefinery 13:4393–4411.
688 https://doi.org/10.1007/s13399-022-03467-0

689 Rathinavelu R, Arumugam E, Paramathma BS (2022) Suitability examination of a new
690 cellulosic fiber extracted from the stem of Ventilago maderaspatana plant as polymer
691 composite reinforcement. Polym Compos 43:3015–3028.
692 https://doi.org/10.1002/pc.26596

693 Rathinavelu R, Paramathma BS (2022) Comprehensive characterization of Echinochloa
694 frumentacea leaf fiber as a novel reinforcement for composite applications. Polym
695 Compos 43:5031–5046. https://doi.org/10.1002/pc.26775

696 Rathinavelu R, Paramathma BS (2023) Examination of characteristic features of raw and
697 alkali-treated cellulosic plant fibers from Ventilago maderaspatana for composite
698 reinforcement. Biomass Convers Biorefinery 13:4413–4425.
699 https://doi.org/10.1007/s13399-022-03461-6

700 Saha A, Kulkarni ND, Kumari P (2023) Development of Bambusa tulda-reinforced different
701 biopolymer matrix green composites and MCDM-based sustainable material selection
702 for automobile applications. Environ Dev Sustain. https://doi.org/10.1007/s10668-023-
703 04327-1

704 Saha A, Kumar S, Kumar A (2021a) Influence of pineapple leaf particulate on mechanical,
705 thermal and biodegradation characteristics of pineapple leaf fiber reinforced polymer
706 composite. J Polym Res 28:66. https://doi.org/10.1007/s10965-021-02435-y

707 Saha A, Kumar S, Zindani D (2021b) Investigation of the effect of water absorption on
708 thermomechanical and viscoelastic properties of flax-hemp-reinforced hybrid composite.
709 Polym Compos 42:4497–4516. https://doi.org/10.1002/pc.26164

710 Saha A, Kumar S, Zindani D, Bhowmik S (2021c) Micro-mechanical analysis of the
711 pineapple-reinforced polymeric composite by the inclusion of pineapple leaf
712 particulates. Proc Inst Mech Eng Part L J Mater Des Appl 235:1112–1127.
713 https://doi.org/10.1177/1464420721990851

714 Saha A, Kumari P (2022) Functional fibers from Bambusa tulda (Northeast Indian species)
715 and their potential for reinforcing biocomposites. Mater Today Commun 31:103800.
716 https://doi.org/10.1016/j.mtcomm.2022.103800

717 Sanjay MR, Madhu P, Jawaid M, et al (2018) Characterization and properties of natural fiber
718 polymer composites: A comprehensive review. J Clean Prod 172:566–581.
719 https://doi.org/10.1016/j.jclepro.2017.10.101

720 Sanjay MRR, Siengchin S, Parameswaranpillai J, et al (2019) A comprehensive review of
721 techniques for natural fibers as reinforcement in composites: Preparation, processing and
722 characterization. Carbohydr Polym 207:108–121.
723 https://doi.org/10.1016/j.carbpol.2018.11.083

724 Sanjeevi R, Jafrey Daniel James D, Senthamaraikannan P (2024) Exploration of
725 Cymbopogon nardus root fibers characteristics for sustainable lightweight composite
726 reinforcement applications. Cellulose 31:9233–9252. https://doi.org/10.1007/s10570-
727 024-06160-9

728 Saravanakumaar A, Senthilkumar A, Saravanakumar SS, et al (2018) Impact of alkali
729 treatment on physico-chemical, thermal, structural and tensile properties of Carica
730 papaya bark fibers. Int J Polym Anal Charact 23:529–536.
731 https://doi.org/10.1080/1023666X.2018.1501931

732 Saravanakumar SSS, Kumaravel A, Nagarajan T, et al (2013) Characterization of a novel
733 natural cellulosic fiber from Prosopis juliflora bark. Carbohydr Polym 92:1928–1933.

https://doi.org/10.1016/j.carbpol.2012.11.064

Saravanan N, Ganeshan P, Prabu B, et al (2022) Physical, Chemical, Thermal and Surface Characterization of Cellulose Fibers Derived from Vachellia Nilotica Ssp. Indica Tree Barks. J Nat Fibers 19:6934–6946. https://doi.org/10.1080/15440478.2021.1941482

Segal L, Creely JJ, Martin AE, Conrad CM (1959) An Empirical Method for Estimating the Degree of Crystallinity of Native Cellulose Using the X-Ray Diffractometer. Text Res J 29:786–794. https://doi.org/10.1177/004051755902901003

Senthamaraikannan P, Kathiresan M (2018a) Characterization of raw and alkali treated new natural cellulosic fiber from Coccinia grandis.L. Carbohydr Polym 186:332–343. https://doi.org/10.1016/j.carbpol.2018.01.072

Senthamaraikannan P, Kathiresan M (2018b) Characterization of raw and alkali treated new natural cellulosic fiber from Coccinia grandis.L. Carbohydr Polym 186:332–343. https://doi.org/10.1016/j.carbpol.2018.01.072

Senthamaraikannan P, Saravanakumar SS (2023) Evaluation of characteristic features of untreated and alkali-treated cellulosic plant fibers from Mucuna atropurpurea for polymer composite reinforcement. Biomass Convers Biorefinery 13:11295–11309. https://doi.org/10.1007/s13399-022-03736-y

Senthamaraikannan P, Saravanakumar SS (2022) Utilization of Mucuna atropurpurea stem fiber as a reinforcement in fiber reinforced plastics. Polym Compos 43:4959–4978

Shibly MAH, Islam MI, Rahat MNH, et al (2024) Extraction and characterization of a novel cellulosic fiber derived from the bark of Rosa hybrida plant. Int J Biol Macromol 257:128446. https://doi.org/10.1016/j.ijbiomac.2023.128446

Siva R, Valarmathi TN, Palanikumar K, Samrot A V (2020) Study on a Novel natural

cellulosic fiber from Kigelia africana fruit: Characterization and analysis. Carbohydr Polym 244:116494. https://doi.org/10.1016/j.carbpol.2020.116494

Srisuk R, Techawinyutham L, Vinod A, et al (2023) Agro-waste from Bambusa flexuosa stem fibers: A sustainable and green material for lightweight polymer composites. J Build Eng 73:106674. https://doi.org/10.1016/j.jobe.2023.106674

Stalin A, Mothilal S, Vignesh V, et al (2021) Mechanical Properties of Typha Angustata/ Vetiver/Banana Fiber Mat Reinforced Vinyl Ester Hybrid Composites. J Nat Fibers. https://doi.org/10.1080/15440478.2021.1875366

Sumrith N, Techawinyutham L, Rapeephun MRS, Suchart D (2020) Characterization of Alkaline and Silane Treated Fibers of ‘ Water Hyacinth Plants ’ and Reinforcement of ‘ Water Hyacinth Fibers ’ with Bioepoxy to Develop Fully Biobased Sustainable Ecofriendly Composites. J Polym Environ. https://doi.org/10.1007/s10924-020-01810-y

Tiwari YM, Sarangi SK (2022) Characterization of raw and alkali treated cellulosic Grewia Flavescens natural fiber. Int J Biol Macromol 209:1933–1942. https://doi.org/10.1016/j.ijbiomac.2022.04.169

Umashankaran M, Gopalakrishnan S (2021) Effect of Sodium Hydroxide Treatment on Physico-chemical, Thermal, Tensile and Surface Morphological Properties of Pongamia Pinnata L . Bark Fiber. J Nat Fibers 18:2063–2076. https://doi.org/10.1080/15440478.2019.1711287

Vijay R, Lenin Singaravelu D, Vinod A, et al (2019) Characterization of raw and alkali treated new natural cellulosic fibers from Tridax procumbens. Int J Biol Macromol 125:99–108. https://doi.org/10.1016/j.ijbiomac.2018.12.056

Vijaya Kumar K, Arul Marcel Moshi A, Selwin Rajadurai J (2020) Mechanical property

780 analysis on bamboo-glass fiber reinforced hybrid composite structures under different
781 lamina orders. Mater Today Proc. https://doi.org/10.1016/j.matpr.2020.08.423

782 Vinod A, Vijay R, Lenin Singaravelu D, et al (2020) Effect of alkali treatment on
783 performance characterization of Ziziphus mauritiana fiber and its epoxy composites. J
784 Ind Text 51:2444S-2466S. https://doi.org/10.1177/1528083720942614

785 Vinod, Rangappa SM, Srisuk R, et al (2023) Agro-waste Capsicum Annum stem: An
786 alternative raw material for lightweight composites. Ind Crops Prod 193:116141.
787 https://doi.org/10.1016/j.indcrop.2022.116141

788 Wu S, Zhang J, Li C, et al (2021) Characterization of potential cellulose fiber from cattail
789 fiber: A study on micro/nano structure and other properties. Int J Biol Macromol
790 193:27–37. https://doi.org/10.1016/j.ijbiomac.2021.10.088

791